IEEE Access
Multidisciplinary | Rapid Review | Open Access Journal

Received April 21, 2022, accepted May 3, 2022, date of publication May 11, 2022, date of current version May 18, 2022.

Digital Object Identifier 10.1109/ACCESS.2022.3173252

Study on the Position Estimation Method of Winding Segmented Permanent Magnet Linear Motor

JIAXI LIU, JIWEI CAO, ZHENGXING CHENG, AND LIYI LI
Harbin Institute of Technology, Harbin, Heilongjiang 150001, China

Corresponding author: Liyi Li (liliyi1024@gmail.com)

This work was supported by the National Natural Science Foundation of China under Grant 51877053.

ABSTRACT The inductance and flux of the winding segmented permanent magnet linear motor(WS-PMLM) change sharply between segments area, so it is difficult to detect the position of the WS-PMLM. In order to solve this problem, this paper presents a method for detecting the mover position of WS-PMLM based on disturbance observer by the compound back EMF. In this paper, a mathematical model of the motor considering the variation of electromagnetic parameters between segments is established and the expressions of the back EMF in the segment and intersegment regions are obtained. Secondly, a method for detecting the position of WS-PMLM based on disturbance observer is proposed. Thirdly, a method to estimate the position between segments is proposed by using the compound back EMF of two adjacent stator segments. Finally, the correctness and effectiveness of the proposed methods are verified by simulation and experiment.

INDEX TERMS Winding segmented permanent magnet linear motor, sensorless, disturbance observer.

I. INTRODUCTION

Winding segmented permanent magnet linear motor is different from ordinary linear motor. Its mover is permanent magnet, so it is not affected by cable drag and can improve the reliability of the motor; The mass of the mover can be small, and the high speed of the linear motor can be realized; Therefore, the motor is suitable for linear motion with high speed and high power. At present, it is widely used in some occasions. However, the disadvantage of this motor is that the stator is composed of winding coils, and its stator needs a long wiring. At the same time, the wiring will be greatly affected. Because only part of the stator and mover of the motor are in contact, and the rest do not work, the efficiency of the motor is greatly reduced. Therefore, the working mode of multi section power supply is usually adopted. Usually, this segmentation will increase the complexity of the circuit, and it is difficult to maintain the stable position of the motor in the inter segment area of the segmentation.

The WS-PMLM has the advantages of high thrust density, small power loss, long stroke, high speed, fast dynamic response and low driving voltage, which has a lot of application prospect in rail transit, electromagnetic launch, new energy and other fields [1]–[5]. However, the position sensor in the WS-PMLM, especially in high-speed and long-stroke applications, cannot be installed due to the cost, maintenance difficulty, volume size and working environment. Therefore, more and more research had been carried out on sensorless control of the WS-PMLM [2]–[4].

In the conventional permanent magnet linear motor system where the mover is the coil winding, the sensorless method usually adopts the flux observer method, the model reference adaptive method, the extended Kalman filter method, the sliding mode observer method and so on [6]–[10].

The position and velocity of the mover are estimated by all kinds of the observer method. However, the sensorless control method is more challenging for the WS-PMLM. The main reason is that the inductance and flux changed between the segments and is coupled with different mover position between the segments, which will also make a great effect on the back EMF. Therefore, it is a difficult problem for WS-PMLM to accurately and effectively estimate the position of movers between segments area.

At present, some scholars have done some research on the sensorless control of WS-PMLM. In the literature [15], the relationship between the electromagnetic parameters and

The associate editor coordinating the review of this manuscript and approving it for publication was Kan Liu.

the secondary position during the primary and secondary coupling transition of the SW-PMLSM is analyzed, a SW-PMLSM high-efficiency V/f control method is proposed which combines the advantages of traditional V/f control and field-oriented control. Literature [12] introduces a general mathematical modeling of the end-effect. Based on such model, modified position observers are proposed for sensorless control using pulsating or rotating voltage vectors. In the literature [13], the main contribution of this paper is to compensate for the angle error caused by the end effect of the linear motor. A mathematical model considering the end effect of the linear motor is constructed to quantitatively analyze the relationship between the position estimation error and the mover position, and the corresponding compensation method is given, and a simplified integral controller is used to estimate the motor position. Literature [14] proposes a method to continuously estimate mover speed and position even during transitions between segments. This method uses an EMF observer for the mover's current position and subsequent segments. Then, based on the observed EMF, a speed and position observer is implemented for the mover.

From the literature on WS-PMLM sensorless control, it can be seen that the sensorless control of the WS-PMLM requires that the mover can be accurately estimated in the full stroke area, especially in the transition region between segments. A more accurate mathematical model and control model within the full stroke are established, and a speed and position estimation method with higher estimation accuracy and better stability in the transition region between segments is found, and a speed and position estimation method suitable for the full travel is established.

Therefore, it is necessary to study the position estimation of the WS-PMLM in the full stroke. Focusing on the relationship between the estimated mover position and the motor parameters of different segments in the transition region between segments, a method of using adjacent segment windings to compound the flux linkage is proposed to solve the position error caused by the simultaneous coupling of the mover and the primary windings of different segments.

In this paper, the estimation of the mover position of WS-PMLM is presented. Firstly, a mathematical model of the WS-PMLM with the variation of electromagnetic parameters between segments is established and the expressions of the EMF in the segment and between segments are derived. Secondly, a method for detecting the mover position of WS-PMLM based on disturbance observer is proposed. Thirdly, the mover position between segments is estimated by the back EMF with two adjacent stator segments. Finally, the correctness and effectiveness of the proposed method are verified by simulation and experiment.

II. MATHEMATICAL MODEL OF WS-PMLM

The length of the secondary and each primary of the WS-PMLM, as well as the gap between the primary sections, can be determined according to the performance, cost and reliability of the motor. In this paper, the primary WS-PMLM with no gap between segments is used. The structure diagram is shown in Figure 1. The primary winding is divided into several segments, and the secondary length is less than the primary length of each segment.

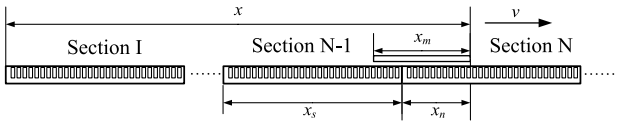

FIGURE 1. Structure of WS-PMLM.

There are three relationships between the secondary and primary windings in the WS-PMLM.

(1) The mover is not coupled with primary winding. There is no energy conversion in this primary winding.

(2) The mover is completely coupled with the primary winding (in the segments). The inductance and flux are constant.

(3) The mover comes in or goes off the primary winding(between segments). The mover is coupled with different primary windings at the same time, and the inductance and flux change with the position of the mover.

The mathematical model of inductance and flux in the WS-PMLM can be expressed as follows:

$$L_s(x) = \begin{cases} L_{s\sigma} + L_m \cdot \frac{x-(n-1)x_s}{x_m} & (n-1)x_s < x \le (n-1)x_s + x_m \\ L_{s\sigma} + L_m & (n-1)x_s + x_m < x \le nx_s \\ L_{s\sigma} + L_m - L_m \cdot \frac{x-nx_s}{x_m} & nx_s < x \le nx_s + x_m \\ L_{s\sigma} & x > nx_s + x_m \end{cases} \tag{1}$$

$$\boldsymbol{\psi}_f(x) = \begin{cases} \psi_f \cdot \frac{x-(n-1)x_s}{x_m} e^{j\frac{\pi}{\tau}x} & (n-1)x_s < x \le (n-1)x_s + x_m \\ \psi_f e^{j\frac{\pi}{\tau}x} & (n-1)x_s + x_m < x \le nx_s \\ \left(\psi_f - \psi_f \cdot \frac{x-nx_s}{x_m}\right) e^{j\frac{\pi}{\tau}x} & nx_s < x \le nx_s + x_m \\ 0 & x > nx_s + x_m \end{cases} \tag{2}$$

Where, n— Number of stator segments, L_m— magnetizing inductance, $L_{s\sigma}$— leakage inductance, ψ_f— magnet flux amplitude.

Compared with the conventional linear motor, the inductance and flux model of the WS-PMLM varies with the mover position. In order to simplify the mathematical model, the inductance and flux linkage of the WS-PMLM are expressed by LS (x) and ψ f (x) respectively.

The voltage equation of WS-PMLM in static system is as follows

$$\boldsymbol{u}_s = R_s \boldsymbol{i}_s + L_s(x)\frac{\mathrm{d}\boldsymbol{i}_s}{\mathrm{d}t} + \boldsymbol{e} \tag{3}$$

According to Figure 1, when the mover is in the region between the n-1 segment and the n segment, two different

stator voltage equations is described in the WS-PMLM.

$$n-1\ segment\begin{cases}\boldsymbol{u}_1 = R_s\boldsymbol{i}_1 + L_{1s}(x)\dfrac{\mathrm{d}\boldsymbol{i}_1}{\mathrm{d}t} + \boldsymbol{e}_1\\ \boldsymbol{e}_1 = \dfrac{\mathrm{d}\boldsymbol{\psi}_1}{\mathrm{d}t} = j\dfrac{\pi v}{\tau}\boldsymbol{\psi}_1 - v\dfrac{\boldsymbol{\psi}_1+\boldsymbol{\psi}_2}{x_m}\end{cases} \tag{4}$$

$$n\ segment\begin{cases}\boldsymbol{u}_2 = R_s\boldsymbol{i}_2 + L_{2s}(x)\dfrac{\mathrm{d}\boldsymbol{i}_2}{\mathrm{d}t} + \boldsymbol{e}_2\\ \boldsymbol{e}_2 = \dfrac{\mathrm{d}\boldsymbol{\psi}_2}{\mathrm{d}t} = j\dfrac{\pi v}{\tau}\boldsymbol{\psi}_2 + v\dfrac{\boldsymbol{\psi}_1+\boldsymbol{\psi}_2}{x_m}\end{cases} \tag{5}$$

where, $\boldsymbol{\psi}_1 = \left(\psi_f - \psi_f\cdot\frac{x_n}{x_m}\right)e^{j\frac{\pi}{\tau}x}$ is flux in the n-1 segment winding, $\boldsymbol{\psi}_2 = \psi_f\left(\frac{x_n}{x_m}\right)e^{j\frac{\pi}{\tau}x}$ is flux in the n segment winding, x_n is the distance between the mover and the n-th segment, $x_n = x-(n-1)x_s$.

$\boldsymbol{\psi}_1$ and $\boldsymbol{\psi}_2$ is substituted into the equations (4) and (5), the EMF can be expressed.

$$\begin{aligned}\boldsymbol{e}_1 &= v\frac{\psi_f}{x_m}\sqrt{1+\frac{\pi^2}{\tau^2}(x_m-x_n)^2}e^{j(\frac{\pi}{\tau}x+\frac{\pi}{2}-\varphi_1)}\\ \boldsymbol{e}_2 &= v\frac{\psi_f}{x_m}\sqrt{1+\frac{\pi^2}{\tau^2}x_n^2}e^{j(\frac{\pi}{\tau}x+\frac{\pi}{2}+\varphi_2)}\end{aligned} \tag{6}$$

where,$\varphi_1 = \arctan\left[\tau/\pi\,(x_m-x_n)\right]$, $\varphi_2 = \arctan(\tau/\pi x_n)$. Assumed $E(u) = v\frac{\psi_f}{x_m}\sqrt{1+\frac{\pi^2}{\tau^2}u^2}$, (6) can be expressed.

$$\begin{aligned}\boldsymbol{e}_1 &= E(x_m-x_n)\,e^{j(\frac{\pi}{\tau}x+\frac{\pi}{2}-\varphi_1)}\\ \boldsymbol{e}_2 &= E(x_n)\,e^{j(\frac{\pi}{\tau}x+\frac{\pi}{2}+\varphi_2)}\end{aligned} \tag{7}$$

From formula (7), the mover position and EMF in the WS-PMLM are very different from linear motor. The following conclusions can be drawn:

(1) In the area between segments, the angle of the back EMF of each segment is no longer the leading mover electrical angle $\pi/2$.

(2) The amplitude of the back EMF of the exit section and the entry section is a function of the mover position and is symmetrical about the center position between the sections. When the position of the mover's midpoint is at the junction between segments, the position deviation is maximum, that is, $\Delta\theta_{r\max} = \arctan\left[\tau/\pi\,(x_m/2)\right]$.

(3) Compared with the intra-segment back EMF, not only the amplitude is attenuated, but also the phase is deviated.

III. THE MOVER POSITION ESTIMATION OF WS-PMLM BASED ON DISTURBANCE OBSERVER

From formula (7), it can be seen that the mover position and back-EMF are the constant of the expression when the mover is completely coupled with the primary winding, which can be estimated by the state observer ways. However, between the segment region, the mover position and back-EMF are a function of the amplitude and phase, which can not be directly used.

Try to Combining the two parts of the flux between different segments in the formula (7), the composite flux can be expressed as

$$\begin{aligned}\boldsymbol{\psi} &= \boldsymbol{\psi}_1+\boldsymbol{\psi}_2 = \left(\psi_f-\psi_f\cdot\frac{x_n}{x_m}\right)e^{j\frac{\pi}{\tau}x} + \psi_f\left(\frac{x_n}{x_m}\right)e^{j\frac{\pi}{\tau}x}\\ &= \psi_f e^{j\frac{\pi}{\tau}x}\end{aligned} \tag{8}$$

It can be seen from formula (8) that although the flux of each stator segment changes with the mover position, the compound flux of the two stator segments remains constant. Similarly, the compound back EMF in the inter-segment also remains constant.

$$\boldsymbol{e} = \boldsymbol{e}_1+\boldsymbol{e}_2 = j\frac{\pi v}{\tau}(\boldsymbol{\psi}_1+\boldsymbol{\psi}_2) = j\frac{\pi v}{\tau}\boldsymbol{\psi} = \frac{\pi v}{\tau}\psi_f e^{j(\frac{\pi}{\tau}x+\frac{\pi}{2})} \tag{9}$$

The compound back EMF eliminates the mutual influence of the magnetic flux generated by the mover in different primary windings, and is the same as the expression of the stator back EMF in the segment, and can be used for position estimation between segments.

DESIGN OF DISTURBANCE OBSERVER

Considered the coupling effect between the mover and only a certain primary winding, a disturbance observer is proposed to estimate the mover position. In order to construct the disturbance observer, the back EMF in formula (3) is regarded as the disturbance, and it is assumed that the state equation and output equation of the WS-PMLM system including the back EMF state variables are as follows.

$$\begin{aligned}\frac{\mathrm{d}}{\mathrm{d}t}\begin{bmatrix}\boldsymbol{i}_s\\ \boldsymbol{e}\end{bmatrix} &= \begin{bmatrix}A_{11} & A_{12}\\ 0 & 0\end{bmatrix}\begin{bmatrix}\boldsymbol{i}_s\\ \boldsymbol{e}\end{bmatrix} + \begin{bmatrix}B_1\\ 0\end{bmatrix}\boldsymbol{u}_s\\ \boldsymbol{i}_s &= \begin{bmatrix}I & 0\end{bmatrix}\cdot\begin{bmatrix}\boldsymbol{i}_s\\ \boldsymbol{e}\end{bmatrix}\end{aligned} \tag{10}$$

In the formula, I is unit array. $A_{11} = -(R_s/L_s)I = a_{11}I$, $A_{12} = -(1/L_s)I = a_{12}I$, $B_1 = (1/L_s)I = b_1 I$.

Using the output deviation $\tilde{\boldsymbol{i}}_s = \hat{\boldsymbol{i}}_s - \boldsymbol{i}_s$, the disturbance observer can be established

$$\dot{\hat{\boldsymbol{i}}}_s = A_{11}\hat{\boldsymbol{i}}_s + A_{12}\hat{\boldsymbol{e}} + B_1\boldsymbol{u}_s + A_{11}(\boldsymbol{i}_s-\hat{\boldsymbol{i}}_s) \tag{11}$$

$$\dot{\hat{\boldsymbol{e}}} = G\left(\hat{\boldsymbol{i}}_s-\boldsymbol{i}_s\right) = A_{12}G\hat{\boldsymbol{e}} + A_{11}G\boldsymbol{i}_s + B_1G\boldsymbol{u}_s - G\dot{\boldsymbol{i}}_s \tag{12}$$

In the formula, G——observer feedback gain matrix, $G = g_1 I$;$\hat{\boldsymbol{e}}$——observe the inverse potential.

The observer error equation can be obtained from formula (10) and formula (12)

$$\dot{\tilde{\boldsymbol{e}}} = \dot{\hat{\boldsymbol{e}}} - \dot{\boldsymbol{e}} = A_{12}G\tilde{\boldsymbol{e}} = -\alpha\tilde{\boldsymbol{e}} \tag{13}$$

In the formula, $\tilde{\boldsymbol{e}}$——inverse potential observation error,$\tilde{\boldsymbol{e}} = \hat{\boldsymbol{e}} - \boldsymbol{e}$, -$\alpha$——observer pole, $\alpha = -a_{12}g_1 = g_1/L_s$.

To satisfy the state observer stability condition, the error of the back EMF satisfies the following condition: For any initial condition $\tilde{\boldsymbol{e}}(0)$, there is $\lim_{t\to\infty}\tilde{\boldsymbol{e}}(t) = 0$. Using the Lyapunov Law, and according to the back-EMF error equation, the Lyapunov function is defined as:

$$V = \frac{1}{2}\tilde{e}_\alpha^2 + \frac{1}{2}\tilde{e}_\beta^2 \tag{14}$$

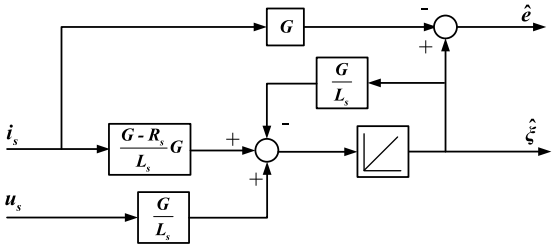

FIGURE 2. Schematic diagram of disturbance observer.

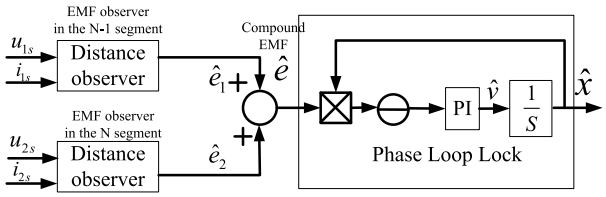

FIGURE 3. The mover estimation between segments.

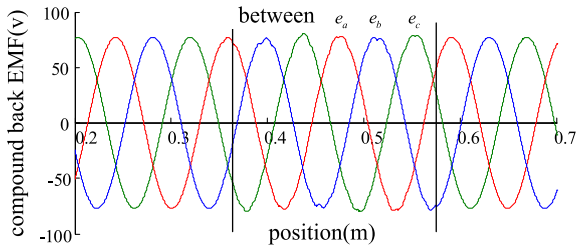

FIGURE 4. The waveform of the compound EMF.

where, $\tilde{e}_\alpha$ and $\tilde{e}_\beta$ are the EMF in the $\alpha\beta$-axis. The derivation of the Lyapunov function is

$$\dot{V} = \tilde{e}_\alpha \cdot \dot{\tilde{e}}_\alpha + \tilde{e}_\beta \cdot \dot{\tilde{e}}_\beta = -\frac{g_1}{L_s}\left(\tilde{e}_\alpha^2 + \tilde{e}_\beta^2\right) \tag{15}$$

To ensure the stability of the observer, let feedback gain $g_1 > 0$. Then $\dot{V}$ is negative definite. According to the Lyapunov Law, the designed disturbance observer is stable.

However, the constructed disturbance observer equation (13) contains the derivative term of current, which will bring great noise in practical application. Therefore, it is necessary to improve the observer equation and introduce new state variables

$$\begin{aligned} \hat{\boldsymbol{\xi}} &= \hat{\boldsymbol{e}} + G\boldsymbol{i}_s \\ \dot{\hat{\boldsymbol{\xi}}} &= \dot{\hat{\boldsymbol{e}}} + G\dot{\boldsymbol{i}}_s \end{aligned} \tag{16}$$

Substitute into equation (13), it can be obtained:

$$\begin{aligned} \dot{\hat{\boldsymbol{\xi}}} &= A_{12}G\hat{\boldsymbol{\xi}} + B_1 G\boldsymbol{u}_s + G\left(A_{11} - A_{12}G\right)\boldsymbol{i}_s \\ \hat{\boldsymbol{e}} &= \hat{\boldsymbol{\xi}} - G\boldsymbol{i}_s \end{aligned} \tag{17}$$

Formula (16) is the enhanced disturbance observer equation, which eliminates the derivative term of the current and is more suitable for practical applications. It is shown in Fig.2.

So the mover position and back-EMF are the constant of the expression when the mover is completely coupled with the primary winding, which can be estimated by the disturbance observer above. However, between the segment region, the mover position and back-EMF are a function of the amplitude and phase, which can not be directly used.

Note that the compound EMF and the compound flux linkage are unchanged in formula 8 and formula 9. The compound EMF could be used to estimate the mover position estimation between segment area. The principle block diagram of the position estimation between segments using the compound back EMF is shown in Figure 3. Between segment area, the back EMF of the two adjacent winding segments are estimated separately, and the two back EMF are combined, and the mover position is estimated by the disturbance observer from the compound back EMF.

The compound back-EMF waveform between segments is shown in Figure 4.

TABLE 1. The parameter in the simulation of servo system.

System parameter	Value
Motor rated speed(m/s)	2
Motor rated voltage(V)	310
Motor pair poles	3
Stator inductance Ls（mH）	35
Stator resistance Rs(Ω)	1.5
Motor inertia Jm（kg·m2）	1.53×10-3
Load thrust（N）	200
Switching frequency（kHz）	10

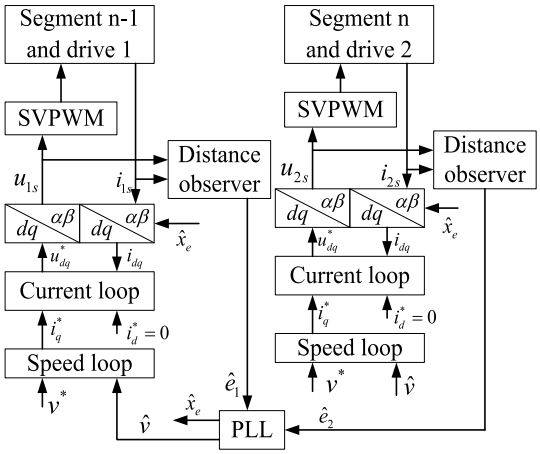

FIGURE 5. The mover estimation application between segments.

IV. SIMULATION

In order to verify the mover position estimation method proposed by compound back EMF between segment windings, a simulation model is built. The parameters of the motor are shown in Table 1.

The application of the mover position estimation is given in the fig.5 between segments. The observed compound back EMF between the segments is shown in figure 6, the mover is in the I segment winding at 0∼0.18s, at this time only the observed back EMF of the I segment winding. The mover is at 0.18s∼0.32s, in the inter-segment area, both the segment I and the segment II have observed back EMF. The mover is

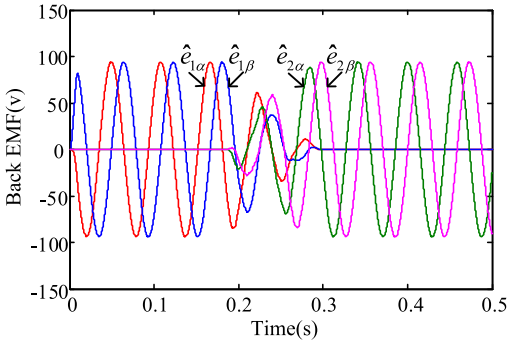

a) the respective mover back EMF in the segments

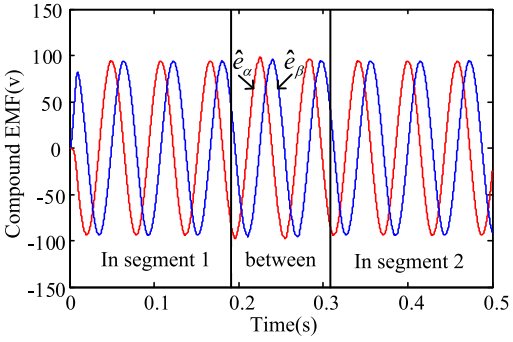

b) the compound mover back EMF in the segments

FIGURE 6. The back EMF estimation.

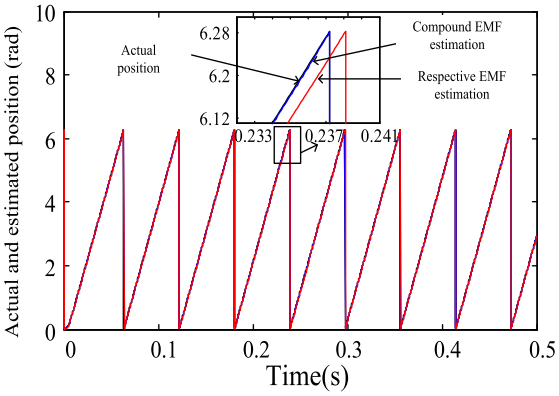

a) actual position and estimated position

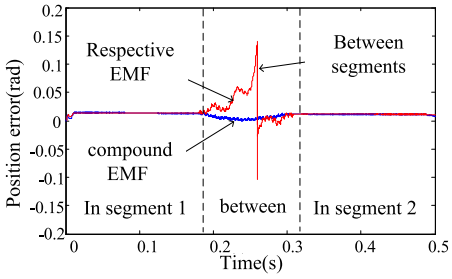

b) position error in the different area

FIGURE 7. Position estimation based on the different back EMF.

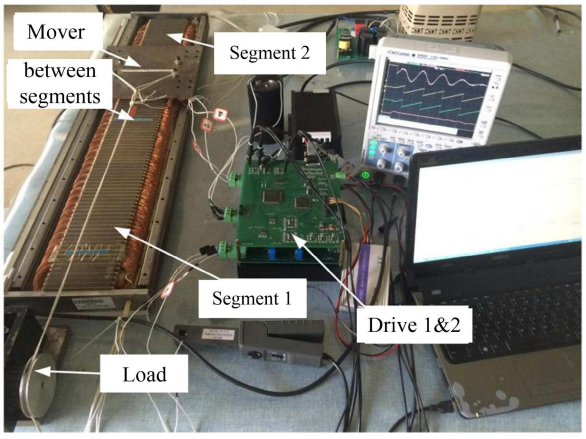

FIGURE 8. The experiment platform in the WS-PMLM drive.

in the inner segment of the stator segment II at 0.32s∼0.5s. At this time, only the observed back EMF of segment II is available.

It can be seen that there is no position deviation between the compound back EMF and the observed back EMF in the segment, which is consistent with the theoretical analysis, so the compound back EMF can be used to estimate the position between the segments.

A comparison was made between the mover position estimation based on the compound back EMF and the back EMF of each individual segment winding between segments. The simulation results are shown in Figure 7.

In Figure 7, the mover is in the I segment winding at 0∼0.18s, the mover is in the II segment winding at 0.32s∼0.5s, and the mover is at 0.18s∼0.32s between the segments. It can be seen that when the back EMF induced by the each segment winding is used to estimate the mover position, the maximum position estimation error is 0.146rad, which is 8.36°.

And the back EMF by the respective winding is used to estimate the position, there will be a large estimation error. However, the compound back EMF is used to estimate the mover position between the segments, the position error is basically the same as mover all inside in the primary winding. The position estimation error is less than 0.015rad, that is, the mover position estimation based on the compound back-EMF can effectively eliminate the position estimation deviation between segments and improve the accuracy of mover position estimation.

V. EXPERIMENT

In order to verify the effectiveness of the compound back EMF observation based on the disturbance observer, mover position estimation between the segments, an experimental platform for the WS-PMLM is built. The WS-PMLM is divided into two segments, which can be controlled at the same time. The experimental platform is shown in Figure 8. The magnetic grid sensor is equipped in the WS-PMLM to obtain the actual position and speed and compare it with the estimated position and speed.

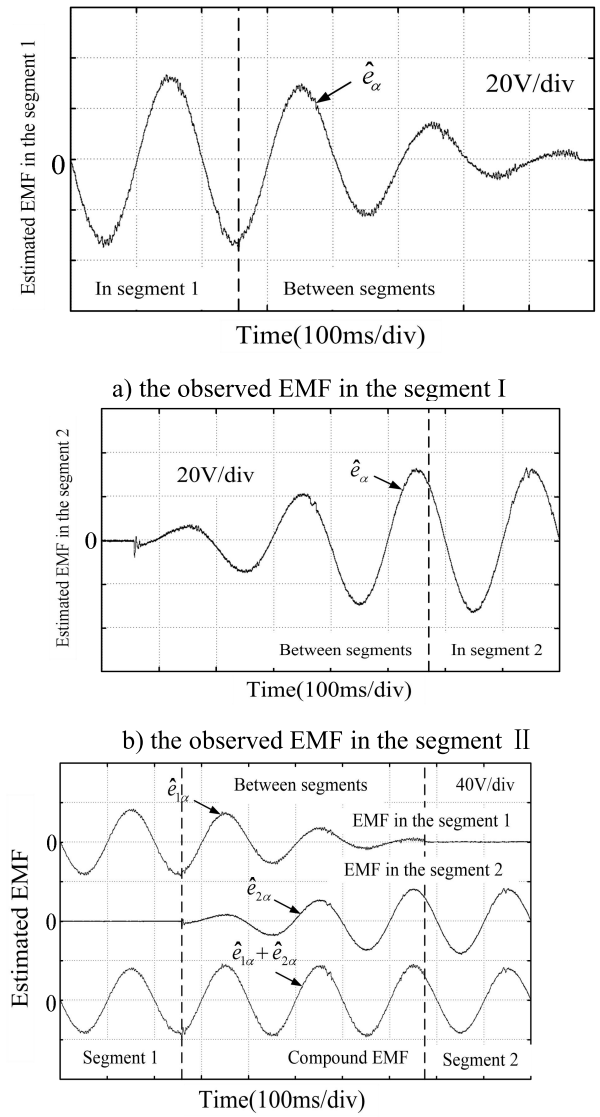

FIGURE 9. The back EMF by the disturbance observer.

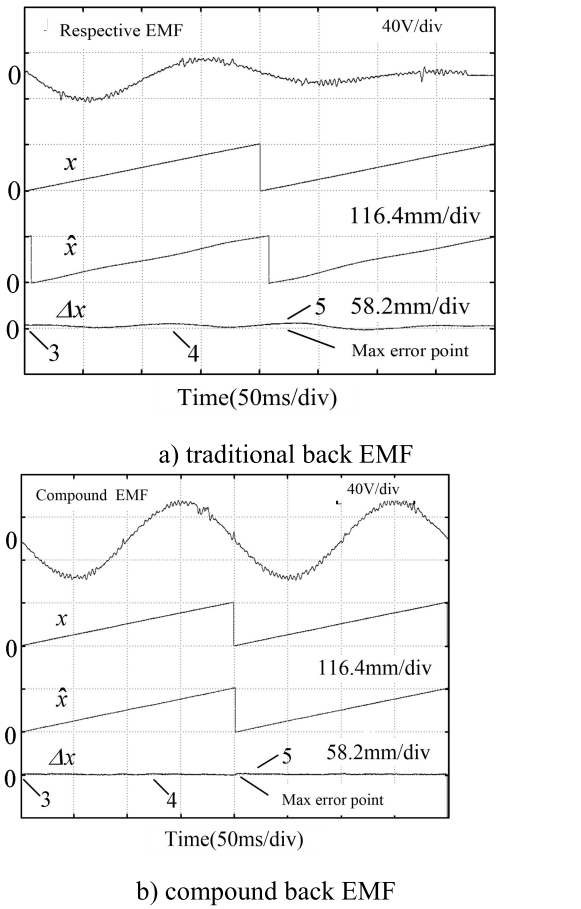

FIGURE 10. The mover position estimation in different method.

TABLE 2. The mover position error in the different ways.

Estimation way	Error In the NO.1 (mm)	Error In the NO.2 (mm)	Error In the NO.3 (mm)	Error In the NO.4 (mm)	Error In the NO.5 (mm)	Error In the max (mm)
respective	1.18	1.15	3.20	5.82	6.54	6.54
compound	0.87	0.98	1.04	0.89	1.16	1.55

The DSP and FPGA can be used in the drive. The disturbance observer, mover position estimation and speed & current closed-loop are applied in the DSP. While, the FPGA is used to perform fault protection, high-speed I/O, and receive AD signals. In this way, the data processing and computing capabilities of the DSP can be used to implement the control algorithm, and the high-speed parallel processing capabilities and high reliability of the FPGA can be used to provide fault protection for the drive.

In the experiment, the speed command is 0.582m/s, that is, the mover frequency is 5Hz (the pole pitch is 58.2mm), and the value of the feedback gain g1=37.8. The amplitude of the observed back EMF within the section is about 30V. The mover runs to the inter-section area, and the magnitude of the observed back EMF gradually decreases until the mover completely exits from section 1.

The observed back-EMF waveform is shown in Figure 9. When the observed back EMF decreases to 0; Figure 9 b) is the observation back EMF in section 2. The amplitude of the observed back EMF gradually increases when the mover enters the section 2, and the mover is completely coupled with the section 2 to observe the back EMF amplitude. Fig. 9c) shows the waveform of the compound back EMF between the segments. It can be seen from the figure that the compound back-EMF observation method based on the disturbance observer can also obtain better performance between segments, which is suitable for the sensorless control of the WS-PMLM.

Figure 10 is the waveform of the mover position estimation by the compound back EMF and traditional back EMF between segments. It can be seen that mover position estimation by using compound back EMF between segments has better performance and has smaller position error. In order to compare the error of the two position estimation methods more clearly, it will be shown as table 2.

In Table 2, points 1 and 2 are located in the area of the segment, and points 3 to 5 are located in the area between the segments. It can be seen that the estimation errors of the two methods for the area within the segment are not much different; the inter-segment area uses the compound back EMF. The estimated error has basically no change compared with the intra-segment area error. The maximum position error is 1.55mm, and the corresponding angle error is 4.8°; the error of the single-segment back EMF estimation in the inter-segment area is greatly increased compared with the intra-segment area error. The maximum position error is 6.54mm, and the corresponding angle error is 20.3°. Compared with the estimation of the single-segment back EMF, the position estimation error of the synthetic back EMF is greatly reduced, which is consistent with the theoretical analysis, which verifies the effectiveness of the inter-segment position estimation method based on the synthetic back EMF.

VI. CONCLUSION

In this paper, a mathematical model of the WS-PMLM considering the transition region between segments is established in the full stroke, and the variation of the mover position with the back EMF and flux linkage of the respective segments in the transition region between segments is obtained. Disturbance observer based on compound EMF method for the WS-PMLM is presented to estimate the mover position. The simulation and experiment is shown that the compound EMF is effectiveness in the sensorless drive. Finally, the correctness and effectiveness of the proposed method are verified by simulation and experiment.

REFERENCES

[1] P. C. Khong, R. Leidhold, and P. Mutschler, "Magnetic guidance of the mover in a long-primary linear motor," *IEEE Trans. Ind. Appl.*, vol. 47, no. 3, pp. 1319–1327, May 2011.
[2] L. Liyi, J. Hong, Z. Lu, L. Ying, Y. Song, L. Rizhong, and L. Xiaopeng, "Fields and inductances of the sectioned permanent-magnet synchronous linear machine used in the EMALS," *IEEE Trans. Plasma Sci.*, vol. 39, no. 1, pp. 87–93, Jan. 2011.
[3] X. Wang, H. Liu, and S. Zhang, "High performance propulsion control of magnetic levitation vehicle long stator linear synchronous motor," in *Proc. Int. Conf. Electr. Mach. Syst.*, Aug. 2011, pp. 1–6.
[4] Y.-J. Kim, H. Dohmeki, and D. Ebihara, "Optimal driving method of stationary discontinuous primary PM-LSM by open-loop control," *IEE Proc., Electr. Power Appl.*, vol. 153, no. 4, p. 585, 2006.
[5] Y.-J. Kim and H. Dohmeki, "Driving method of stationary discontinuous-armature PMLSM by open-loop control for stable-deceleration driving," *IET Electr. Power Appl.*, vol. 1, no. 2, p. 248, 2007.
[6] C. Yang, T. Ma, Z. Che, and L. Zhou, "An adaptive-gain sliding mode observer for sensorless control of permanent magnet linear synchronous motors," *IEEE Access*, vol. 6, pp. 3469–3478, 2018.
[7] X. Sun, M. Wu, C. Yin, S. Wang, and X. Tian, "Multiple-iteration search sensorless control for linear motor in vehicle regenerative suspension," *IEEE Trans. Transport. Electrific.*, vol. 7, no. 3, pp. 1628–1637, Sep. 2021.
[8] H.-W. Zhang, D. Jiang, X.-H. Wang, and M.-R. Wang, "Direct thrust force sensorless control of PMLSM based on dual extended Kalman filter," in *Proc. 13th Int. Symp. Linear Drives Ind. Appl. (LDIA)*, Jul. 2021, pp. 1–6.
[9] T. Wen, Z. Wang, B. Xiang, B. Han, and H. Li, "Sensorless control of segmented PMLSM for long-distance auto-transportation system based on parameter calibration," *IEEE Access*, vol. 8, pp. 102467–102476, 2020.
[10] C. He, S. Shilong, Z. Xueqian, and S. Dali, "Sensorless DPCC of PMLSM using SOGI-PLL based high-order SMO with cogging force feedforward compensation," *IEEE Trans. Transport. Electrific.*, vol. 8, no. 1, pp. 1094–1104, Mar. 2022.
[11] S. Chi, Z. Zhang, and L. Xu, "Sliding-mode sensorless control of direct-drive PM synchronous motors for washing machine applications," *IEEE Trans. Ind. Appl.*, vol. 45, no. 2, pp. 582–590, Mar./Apr. 2009.
[12] T. Bernardes, V. F. Montagner, H. A. Gründling, and H. Pinheiro, "Discrete-time sliding mode observer for sensorless vector control of permanent magnet synchronous machine," *IEEE Trans. Ind. Electron.*, vol. 61, no. 4, pp. 1679–1691, Apr. 2014.
[13] P. Giangrande, F. Cupertino, and G. Pellegrino, "Modelling of linear motor end-effects for saliency based sensorless control," *IEEE Energy Convers. Congr. Expo.*, vol. 2010, pp. 3261–3268.
[14] F. Cupertino, P. Giangrande, G. Pellegrino, and L. Salvatore, "End effects in linear tubular motors and compensated position sensorless control based on pulsating voltage injection," *IEEE Trans. Ind. Electron.*, vol. 58, no. 2, pp. 494–502, Feb. 2011.
[15] R. Leidhold and P. Mutschler, "Speed sensorless control of a long-stator linear synchronous motor arranged in multiple segments," *IEEE Trans. Ind. Electron.*, vol. 54, no. 6, pp. 3246–3254, Dec. 2007.
[16] L. Cui, H. Zhang, and D. Jiang, "Research on high efficiency V/f control of segment winding permanent magnet linear synchronous motor," *IEEE Access*, vol. 7, pp. 138904–138914, 2019.

JIAXI LIU was born in Harbin, China, in 1980. He received the B.E., M.E., and D.E. degrees from the Harbin Institute of Technology (HIT), Harbin, in 2002, 2004, and 2010, respectively. Since 2015, he has been an Associate Professor with the School of Electrical Engineering and Automation, HIT. He holds ten patents. His research interests include high-speed motor drive and linear motor drive.

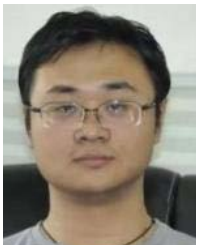

JIWEI CAO was born in Harbin, China, in 1983. He received the B.S. and M.S. degrees in electrical engineering from the Shenyang University of Technology, in 2005 and 2008, respectively, and the Ph.D. degree in electrical engineering from the Harbin Institute of Technology, in 2014. Since 2014, he has been a Research Assistant with the Electrical Engineering Department, Harbin Institute of Technology. He holds 15 patents. His research interests include high-power density permanent magnets motors, high-temperature superconducting motors, high-speed motors, and motors measurement technology.

ZHENGXING CHENG was born in Jinan, Shandong, China, in 1994. He received the B.E. degree and M.S. degrees from Shandong University, Jinan, in 2013 and 2017, respectively, both in electrical engineering. He is currently pursuing the Ph.D. degree in electrical engineering with the Harbin Institute of Technology (HIT), Harbin, China. His research interests include parameter identification, robust control, and model predictive control of PMSM.

LIYI LI received the B.E., M.E., and D.E. degrees from the Harbin Institute of Technology (HIT), Harbin, China, in 1991, 1995, and 2001, respectively. Since 2004, he has been a Professor with the School of Electrical Engineering and Automation, HIT. He became a Yangtze Fund Scholar Distinguished Professor, in 2013. He was supported by the National Science Fund for Distinguished Young Scholars. He has authored or coauthored over 110 technical articles. He holds 50 patents. His research interests include design, drive, and control of linear motors and design and drive of high-speed and high-power density permanent magnet machines.